



Title	Serial Change and Clinical Impact of Irregular Protrusion in Lesions With Chronic Coronary Syndrome
Author(s)	Okamoto, Naotaka; Mizote, Isamu; Ishihara, Takayuki et al.
Citation	Catheterization and Cardiovascular Interventions. 2025
Version Type	VoR
URL	https://hdl.handle.net/11094/100545
rights	This article is licensed under a Creative Commons Attribution-NonCommercial-NoDerivatives 4.0 International License.
Note	

The University of Osaka Institutional Knowledge Archive : OUKA

<https://ir.library.osaka-u.ac.jp/>

The University of Osaka

ORIGINAL ARTICLE - CLINICAL SCIENCE OPEN ACCESS

Serial Change and Clinical Impact of Irregular Protrusion in Lesions With Chronic Coronary Syndrome

Naotaka Okamoto¹  | Isamu Mizote² | Takayuki Ishihara³  | Daisuke Nakamura² | Tatsusya Shiraki²  | Naoki Itaya⁴ | Takuya Tsujimura³  | Mitsuyoshi Takahara⁵ | Shungo Hikosou² | Toshiaki Mano³ | Takahumi Ueno⁶ | Masami Nishino¹  | Shinsuke Nanto⁷ | Yasushi Sakata²

¹Division of Cardiology, Osaka Rosai Hospital, Sakai, Japan | ²Department of Cardiovascular Medicine, Osaka University Graduate School of Medicine, Suita, Japan | ³Kansai Rosai Hospital Cardiovascular Center, Amagasaki, Japan | ⁴Division of Cardiovascular Medicine, Kurume University School of Medicine, Kurume, Japan | ⁵Department of Diabetes Care Medicine, Osaka University Graduate School of Medicine, Suita, Japan | ⁶Division of Cardiology, Fukuoka Memorial Hospital, Fukuoka, Japan | ⁷Department of Cardiovascular Medicine, Nishinomiya Municipal Central Hospital, Nishinomiya, Japan

Correspondence: Isamu Mizote (i-mizote@cardiology.med.osaka-u.ac.jp)

Received: 3 September 2024 | **Revised:** 28 December 2024 | **Accepted:** 17 January 2025

Funding: This study was supported by Abbott Medical Japan, Cardinal Health Japan, Taisho Biomed Instruments Co. Ltd. and Biosensors Japan.

Keywords: chronic coronary syndrome | irregular protrusion | optical coherence tomography

ABSTRACT

Background: The changes over time and effects on long-term clinical outcomes beyond 1 year of irregular protrusion (IP) in chronic coronary syndrome (CCS) remains unclear.

Aims: This study aimed to assess the time-dependent change and long-term clinical impact of IP in CCS lesions.

Methods: This study was a post hoc analysis of COLLABORATION study, which was a multicenter, prospective, observational study conducted from July 2018 to February 2020, assessing 1- and 12-month serial vessel responses after stent implantation using OCT and coronary angiography. Time-dependent change in the presence of IP was evaluated using the serial OCT examinations. The cumulative 3-year incidence of TLR was compared between the lesions with and without IP, as well as between those with and without residual IP at 1 month.

Results: Among 107 lesions, IP was detected in post-OCT pullbacks in 38 (35.5%) lesions. Out of the 38 lesions, IP remained in 9 (23.7%) lesions at 1 month and existed in 2 (5.3%) lesions at 12 months. The cumulative 3-year incidence of TLR was significantly higher in IP group than in non-IP group (13.6% vs. 3.0%, $p = 0.04$). Similarly, it was significantly higher in lesions with residual IP at 1 month than those without (33.3% vs. 4.3%, $p < 0.01$). All residual IP at 1 month were composed of angiographic yellow plaques and red thrombi.

Conclusions: The presence of IP decreased over time, but approximately one-fourth of IP remained at 1 month. IP and residual IP at 1 month were important post-stent OCT findings leading to long-term TLR in patients with CCS.

1 | Introduction

Optical coherence tomography (OCT) is an intravascular imaging device with high resolution and enables detailed observation after stent implantation during percutaneous coronary intervention (PCI). A protrusion of material between struts after stent

implantation is clearly visualized and recognized as tissue protrusion by OCT [1]. While the clinical impact of tissue protrusion has been explored, several previous reports have failed to demonstrate an evident association between tissue protrusion and clinical events [2–5]. However, Soeda et al. classified tissue protrusion into three categories: smooth protrusion, disrupted fibrous tissue protrusion,

Abbreviations: ACS, acute coronary syndrome; CAS, coronary angiography; CCS, chronic coronary syndrome; DES, drug-eluting stent; IP, irregular protrusion; NIC, neointimal coverage; NIH, neointimal hyperplasia; OCT, optical coherence tomography; PCI, percutaneous coronary intervention; TLR, target lesion revascularization.

This is an open access article under the terms of the [Creative Commons Attribution-NonCommercial-NoDerivs](https://creativecommons.org/licenses/by-nc-nd/4.0/) License, which permits use and distribution in any medium, provided the original work is properly cited, the use is non-commercial and no modifications or adaptations are made.

© 2025 The Author(s). *Catheterization and Cardiovascular Interventions* published by Wiley Periodicals LLC.

and irregular protrusion (IP) according to their appearance. IP was defined as tissue protrusion with an irregular surface into the lumen between struts after stent implantation. The smooth protrusion and disrupted fibrous tissue protrusion were not related to clinical events, whereas IP has been reported to be an independent predictor of adverse clinical events at 1 year, particularly target lesions revascularization (TLR), in lesions associated with acute coronary syndrome (ACS), accounting for half of them [6]. Lipid-rich plaque evaluated by OCT has been identified as one of the predictors of IP [7] and is more frequently observed in lesions associated with ACS than in those with chronic coronary syndrome (CCS) [8]. Furthermore, patients with ACS have a worse prognosis [9] and a higher risk for stent thrombosis compared with those with CCS [10]. Therefore, the clinical importance of IP in CCS could be different from that in ACS and it has not been established. Additionally, the changes over time and effects on long-term clinical outcomes beyond 1 year of IP have not been well investigated, either. This study aimed to assess the time-dependent change and clinical impact on long-term outcomes of IP in CCS.

2 | Methods

2.1 | Study Population

The COLLABORATION study was a multicenter, prospective, and observational study assessing vessel responses after new-generation drug-eluting stent (DES) implantation using OCT and coronary angiography (CAS) [11]. It included patients with CCS, multi-vessel disease in a native coronary artery, implantation of a polymer-free and carrier-free biolimus A9-coated stent (BioFreedom, Biosensors Interventional Technologies, Singapore), or a durable polymer everolimus-eluting stent (Xience, Abbott Vascular, Santa Clare, CA, USA) at the initial PCI. The staged PCI for the residual lesion was performed at 1 ± 0.5 months after the initial PCI. All PCI was performed from July 2018 to February 2020. Serial follow-up OCT and CAS examinations were performed at the staged PCI and at 12 ± 2 months after the initial PCI. The study was approved by each hospital's Ethics Committee, and it adhered to the tenets of the Declaration of Helsinki. Written informed consent regarding participation in this study, which included an agreement for OCT and CAS examinations during staged PCI and the 12-month follow-up, was obtained before the initial PCI. Additionally, written informed consent was secured for each procedure: the initial PCI, the staged PCI, and the follow-up CAG. Written informed consent was provided by all patients participated in the study. The detailed study protocol was described elsewhere [11]. Among the lesions included in the COLLABORATION study, the lesions where IP assessment was unavailable were excluded. The remaining lesions were divided into two groups according to the presence of IP in the OCT examination at the initial PCI.

2.2 | OCT Procedure and Analysis

OCT pullbacks were obtained for the initial lesion immediately after PCI, at the staged PCI, and at the 12-month follow-up using OPTIS Mobile System (Abbott Vascular, Santa Clare, CA, USA). After crossing a conventional guidewire distal to the

lesion, the 2.7F frequency domain- OCT catheter (Abbott Vascular, Santa Clare, CA, USA) was advanced beyond the lesion. During the OCT examination, blood was cleared by an injection of contrast dye. The images were calibrated by automated adjustment of the Z-offset and the automated pullback with 25 mm/s was used. Data was obtained using an OCT system (OPTIS Mobile System, Abbott Vascular, Santa Clare, CA, USA) and digitally stored. OCT analysis was performed using off-line software (Off-line Review Software, version E.0.2; Abbott Vascular, Santa Clare, CA, USA). Cross-sectional images with any part of the stent out of the screen, a side branch occupied $> 45^\circ$, or poor quality due to residual blood, an artifact, or reverberations were excluded.

IP was defined as the protrusion of material with an irregular surface into the lumen between struts with maximal height $\geq 100 \mu\text{m}$ as previously reported [6]. The presence of IP was evaluated through serial OCT images in the IP group. When the IP remained at 1 month after the initial PCI, the IP was defined as residual IP.

For post-PCI and follow-up OCT analysis, a qualitative assessment was performed at 1 mm intervals as previously described [11]. The proximal and distal references were measured at the site with the largest lumen within 5 mm proximal and distal to the stent edges. Stent edge dissection was defined as disruption of the vessel lumen surface with a visible flap within 5 mm of the proximal and distal reference segments. The stent expansion index was calculated as the minimum stent cross-sectional area divided by the average of the proximal and distal reference lumen areas multiplied by 100. Struts were classified as embedded, apposed, and malapposed according to the distance between the strut and lumen surface. If any tissue was observed on the strut, the strut was categorized as an embedded strut. If any part of the strut was visibly exposed to the lumen, the strut was defined as an uncovered strut. Furthermore, the uncovered struts were classified as apposed or malapposed struts; malapposed struts were defined as struts with the distance between struts and lumen surface greater than or equal to the axial resolution of OCT plus the width of the stent strut of each stent type including the polymer coating. The embedded distance or neointimal hyperplasia (NIH) thickness was measured as the distance between the endoluminal surface of the struts and the lumen contour. Maximal and mean embedded distance or NIH thickness was calculated for each lesion. NIH was categorized as a low signal pattern or a homogenous high signal pattern; NIH with a low signal pattern was described as having focally changing optical properties and showing various backscattering patterns or consisting of concentric layers with different optical properties, whereas NIH with homogenous high signal pattern was identified as having signal-rich regions with low attenuation [12].

2.3 | CAS Procedure and Analysis

CAS was performed for the initial lesion at the time of the staged PCI and at the 12-month follow-up using Forwardlooking (Taisho Biomed Instruments, Osaka, Japan) or a smart-I angiographic catheter (i Heart Medical, Tokyo, Japan). An optical fiber was advanced to the distal segment of the coronary artery

and then manually pulled back from the distal edge to the proximal edge of the stent. Blood flow was blocked by injecting low-molecular-weight dextran using a guide extension catheter during the image acquirement. Angioscopic images were digitally stored for off-line analysis. Neointimal coverage (NIC) over the stent was classified into four grades, as previously described: grade 0, stent struts fully visible, similar to immediately after implantation; grade 1, transparently visible stent struts bulging into the lumen; grade 2, transparently visible stent struts embedded in the neointima; grade 3, invisible stent struts fully embedded into the neointima. The yellow color grade was evaluated based on the color of plaque and graded as follows: grade 0, white; grade 1, light yellow; grade 2, yellow; grade 3, intense yellow [13]. The thrombus grade showing the adhesion of thrombus was graded as: grade 0, no thrombus; grade 1, several spotty thrombi; and grade 2, thrombus extending between struts [14].

2.4 | Outcomes

Time-dependent change in the presence of IP was evaluated using the serial OCT examinations. OCT and CAS parameters were compared between the two groups. Incidences of clinical outcomes including TLR and target vessel revascularization (TVR) at 3 years were compared between the groups with (IP group) or without IP (non-IP group). TLR was defined as any clinically indicated repeat PCI of the target lesion or bypass surgery of the target vessel performed for restenosis or another complication of the target lesion [15]. Revascularization was considered clinically indicated if angiography at follow-up showed a percent diameter stenosis of 50% or more and if one of the following was present: a positive history of recurrent angina pectoris, objective signs of ischemia at rest or during an exercise test, and abnormal results of any invasive functional diagnostic test [16]. Furthermore, the impact on clinical events of residual IP at 1 month were assessed.

2.5 | Statistical Analysis

Continuous variables are presented as the median (25th percentile–75th percentile) and were compared by the Mann–Whitney test. Categorical variables are presented as numbers and percentages and

were compared using Fisher's exact test. A Kaplan–Meier estimate with a log-rank test was used to compare the TLR and TVR rates between the two groups. A value of $p < 0.05$ was considered statistically significant. Statistical analyses were performed using R version 3.6.0 (R Development Core Team, Vienna, Austria).

3 | Results

3.1 | Time-Dependent Change of the Incidences of IP

Among the 121 lesions, 14 lesions were excluded, because IP assessment was unavailable. The remaining 107 lesions were included in this study. IP was detected in post-OCT pullbacks in 38 (35.5%) lesions. Therefore, IP group consisted of 38 lesions and non-IP group consisted of 69 lesions. Out of the 38 lesions in the IP group, IP remained in 9 (23.7%) lesions at 1 month and still existed in 2 (5.3%) lesions at 12 months (Figure 1).

3.2 | Patient, Lesion, and Procedural Characteristics

Patient characteristics are summarized in Table 1. The age, gender, and prevalence of hypertension, dyslipidemia, and diabetes mellitus were comparable between the two groups. Medication at baseline did not differ between the groups. Table 2 shows lesion and procedural characteristics. The target vessel was similarly located in the two groups. IP group had significantly greater pre-percent diameter stenosis compared with non-IP group (72.1 [63.3%–85.1%] vs. 65.4 [58.3%–75.0%], $p = 0.03$). Procedural characteristics regarding stents and balloons were not different between the two groups.

3.3 | OCT Parameters

In post-OCT parameters, IP group had significantly larger maximum embedded distances (215 [130–318] vs. 130 [70–190 μm], $p < 0.01$) and mean embedded distances (320 [180–410] vs. 265 [200–375 μm], $p < 0.01$) than non-IP group, but the percentages of embedded, apposed, and malapposed struts were similar in the two groups (Table 3). The mean stent

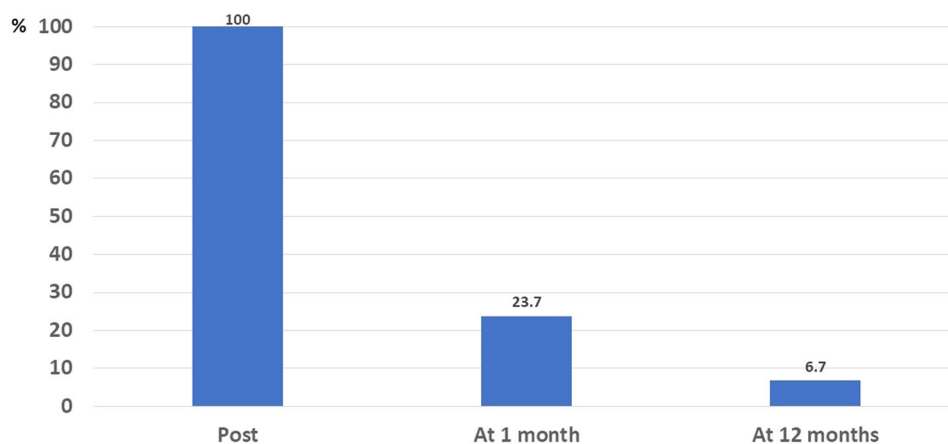


FIGURE 1 | Time-dependent change of presence of irregular protrusion. [Color figure can be viewed at [wileyonlinelibrary.com](https://onlinelibrary.wiley.com)]

TABLE 1 | Patient characteristics.

	IP group (<i>n</i> = 38)	Non-IP group (<i>n</i> = 69)	<i>p</i> value
Age	73.5 (69.3–79.5)	72.0 (68.0–78.0)	0.64
Male, <i>n</i> (%)	32 (84)	59 (86)	> 0.99
Smoker, <i>n</i> (%)	11 (29)	19 (28)	> 0.99
Hypertension, <i>n</i> (%)	32 (84)	51 (74)	0.33
Dyslipidemia, <i>n</i> (%)	37 (97)	66 (96)	> 0.99
Diabetes mellitus, <i>n</i> (%)	18 (47)	31 (45)	0.84
Prior percutaneous coronary intervention, <i>n</i> (%)	16 (42)	18 (26)	0.13
Prior coronary artery bypass graft, <i>n</i> (%)	2 (5)	3 (4)	> 0.99
Atrial fibrillation, <i>n</i> (%)	3 (8)	12 (17)	0.25
Chronic heart disease, <i>n</i> (%)	3 (8)	5 (7)	> 0.99
Cerebral vascular disease, <i>n</i> (%)	3 (8)	10 (14)	0.37
Medication use at the time of initial percutaneous coronary intervention, <i>n</i> (%)			
Aspirin	38 (100)	69 (100)	> 0.99
P2Y12 inhibitor			0.38
Clopidogrel	9 (24)	23 (33)	
Prasugrel	29 (76)	46 (67)	
Anticoagulant			0.16
Direct oral anticoagulant	2 (5)	11 (16)	
Warfarin	0 (0)	1 (1)	
Statin	37 (97)	61 (88)	0.15
Presence of symptoms, <i>n</i> (%)	23 (61)	36 (52)	0.43
Triple vessel disease, <i>n</i> (%)	9 (24)	14 (20)	0.63

Note: Values are the median (interquartile) or *n* (%).
Abbreviation: IP = irregular protrusion.

area was significantly larger in the IP group than in the non-IP group (7.11 [5.21–8.41] vs. 5.92 [4.36–7.50 mm²], *p* = 0.04), while minimal stent area was comparable. The reference area was similar between the two groups. The stent expansion index did not differ between the two groups.

Among the 107 lesions, 1-month OCT was performed for all, while 12-month OCT was conducted for 92 lesions (86%). For follow-up OCT examinations, the percentage of a homogeneous high signal pattern of neointima was significantly greater in the IP group than in non-IP group (50 [27.7%–100%] vs. 32.7 [0%–79.5%], *p* = 0.01) at 1 month, but increased to 100% with no difference between the groups at 12 months (Table 4). The percentage of covered struts was approximately 87% at 1 month and increased to over 99% at 12 months in both groups. The percentage of uncovered apposed struts was 11.8% and 11.7% at 1 month in IP and non-IP groups and decreased to 0.5% at 12 months in both groups. The percentage of uncovered malapposed struts was 1.2% at 1 month and 0% at 12 months in both groups. The mean neointimal thickness was 46 μm at 1 month and increased to more than 100 μm at 12 months in both groups.

3.4 | One- and 12-Month Follow-Up CAS

Of the 107 lesions, 1-month CAS was performed for 105 lesions (98%), while 12-month CAS was conducted for 91 lesions (85%).

CAS findings are shown in Figure 2. All CAS parameters were similarly observed in both groups at 1 month. Approximately 70% of the lesions had a dominant NIC grade of 0, thrombi were detected in almost all lesions, and intensive yellow plaques were detected in approximately half of the lesions. At 12 months, while NIC grades became higher in both groups, minimum NIC grade tended to be lower in IP group than in non-IP group. Thrombus grade and yellow color grade became lower at 12 months, and they were similar between IP and non-IP groups.

3.5 | Association Between IP and 3-Year TLR or TVR

Kaplan–Mayer curves show 3-year TLR and TVR rates according to the presence of IP at the initial PCI or at 1-month follow-up (Figure 3). The TLR rate was 13.6% at 3 years in the IP group, while it was 3.0% in the no-IP group (*p* = 0.04, Figure 3A). The TVR rates were 13.6% in the IP and 8.8% in the no-IP group with no significant difference (Figure 3B). The TLR rates at 3 years were significantly higher in the lesions with residual IP at 1 month than those without (33.3% vs. 4.3%, *p* < 0.01, Figure 3C). The lesions with residual IP at 1 month had a TVR rate of 33.3%, while the lesions without residual IP showed a TVR rate of 8.4% (*p* < 0.01, Figure 3D).

TABLE 2 | Lesion characteristics.

	IP group (n = 38)	Non-IP group (n = 69)	p value
Target vessel, n (%), LAD/LCX/RCA	9 (24)/14 (37)/15 (39)	23 (33)/25 (36)/21 (30)	0.55
Chronic total occlusion, n (%)	4 (11)	1 (1)	0.053
Lesion length, mm	22.5 (12.0–29.8)	24.0 (14.0–32.0)	0.77
Pre-reference vessel diameter, mm	2.55 (2.20–2.98)	2.60 (2.30–3.00)	0.92
Pre minimum lumen diameter, mm	0.70 (0.40–1.08)	0.80 (0.62–1.10)	0.06
Pre percent diameter stenosis, %	72.1 (63.3–85.1)	65.4 (58.3–75.0)	0.03
AHA/ACC classification, n (%), A/B1/B2/C	1 (3)/3 (8)/4 (11)/30 (79)	5 (7)/9 (13)/9 (13)/46 (67)	0.16
Number of stents	1 (1–1)	1 (1–1)	0.69
Biofreedom	18 (47)	42 (61)	0.22
Stent size, mm	2.84 (2.50–3.25)	2.75 (2.50–3.00)	0.41
Stent length, mm	29.0 (24.0–36.0)	28.0 (18.0–38.0)	0.25
Stent pressure, atm	9 (6–12)	8 (6–12)	0.27
Stent size/pre-RVD	1.14 (0.97–1.31)	1.08 (1.00–1.18)	0.30
Predilatation, n (%)	36 (95)	58 (84)	0.13
Pre-balloon size, mm	2.50 (2.00–3.00)	2.50 (2.00–2.75)	0.35
Pre-balloon pressure, atm	12 (12–14)	12 (10–14)	0.61
Postdilatation, n (%)	37 (97)	67 (97)	> 0.99
Post balloon size, mm	3.25 (3.00–3.50)	3.25 (2.75–3.50)	0.44
Post balloon pressure, atm	18 (16–20)	18 (18–20)	0.38

Note: Values are the median (interquartile) or n (%).

Abbreviations: IP = irregular protrusion, LAD = left anterior descending artery, LCX = left circumflex, RCA = right coronary artery, RVD = reference vessel diameter.

TABLE 3 | Post-optical coherence tomography parameters.

	IP group (n = 38)	Non-IP group (n = 69)	p value
Mean reference area, mm ²	6.15 (4.11–7.91)	5.56 (4.18–7.42)	0.60
Distal reference area, mm ²	4.99 (3.26–6.86)	4.80 (3.59–6.57)	0.82
Proximal reference area, mm ²	7.20 (4.94–9.18)	6.81 (5.12–8.51)	0.58
Minimal stent area, mm ²	4.48 (3.67–6.17)	4.49 (3.47–6.08)	0.79
Mean stent area, mm ²	7.11 (5.21–8.41)	5.92 (4.36–7.50)	0.04
Stent expansion index	78 (66–92)	83 (72–93)	0.40
Stent edge dissection, n (%)			
Distal edge	1 (3)	6 (9)	0.26
Proximal edge	4 (11)	10 (15)	0.77
Distal or proximal edge	5 (14)	13 (20)	0.59
Analyzed struts per lesion, n	209 (146–269)	162 (104–262)	0.13
Percentage of struts (%)			
Embedded strut	18.5 (7.5–37.8)	12.4 (7.2–24.5)	0.21
Apposed strut	72.4 (49.6–84.7)	78.3 (70.3–85.9)	0.07
Malapposed strut	2.3 (0.6–9.1)	4.1 (1.3–9.1)	0.52
Maximum embedded distance, μm	215 (130–318)	130 (70–190)	< 0.001
Mean embedded distance, μm	47 (36–79)	32 (26–41)	< 0.001
Maximum malapposed distance, mm	320 (180–410)	265 (200–375)	0.51

Note: Values are the median (interquartile) or n (%).

Abbreviation: IP = irregular protrusion.

TABLE 4 | Follow-up optical coherence tomography findings.

	1 month		12 months		p value	p value
	IP group (n = 38)	Non-IP group (n = 69)	IP group (n = 38)	Non-IP group (n = 69)		
Percentage of covered struts, %	87.1 (71.5–93.2)	86.7 (77.1–95.1)	99.4 (98.3–100.0)	99.5 (97.9–100.0)	0.80	0.89
Percentage of adequate struts, %	45.4 (31.2–57.1)	51.8 (36.9–63.6)	73.3 (62.2–92.9)	84.6 (72.0–92.3)	0.14	0.42
Percentage of uncovered apposed struts, %	11.8 (6.2–22.7)	11.7 (3.2–21.2)	0.5 (0.0–1.4)	0.5 (0.0–1.4)	0.85	0.93
Percentage of uncovered malapposed struts, %	1.2 (0.0–3.2)	1.2 (0.0–3.4)	0.0 (0.0–0.1)	0.0 (0.0–0.0)	0.66	0.87
Maximum malapposed distance, mm	280 (195–450)	320 (210–540)	335 (283–428)	370 (275–520)	0.27	0.58
Maximum neointimal thickness, μm	225 (173–308)	200 (150–250)	445 (300–528)	350 (290–495)	0.14	0.22
Mean neointimal thickness, μm	46 (32–59)	46 (32–65)	100 (63–154)	107 (76–145)	0.68	0.71
Low signal pattern, %	50.0 (0.0–71.4)	67.3 (21.7–100.0)	0.0 (0.0–0.0)	0.0 (0.0–0.0)	0.02	0.38
Homogeneous high signal pattern, %	50.0 (29.6–100.0)	32.7 (0–78.4)	100.0 (94.0–100.0)	100.0 (100.0–100.0)	0.01	0.35
Neointerostclerosis, n (%)	1 (3)	0 (0)	2 (7)	4 (6)	0.36	> 0.99

Note: Values are the median (interquartile) or n (%).
Abbreviation: IP = irregular protrusion.

3.6 | OCT and CAS Images of Residual IP at 1 Month

Figure 4 shows OCT and CAS images of residual IP at 1 month. CAS images were not available in two lesions. All residual IPs at 1 month were composed of angioscopic yellow plaques and red thrombi.

4 | Discussions

The present study was the first report showing the time-dependent change and impact on long-term clinical outcomes of IP in lesions with CCS. The main findings of the study included the following: (1) IP gradually disappeared following the stent implantation; (2) IP was associated with 3-year TLR, and residual IP at 1 month was strongly related to 3-year TLR and TVR in CCS lesions.

OCT-detected tissue protrusion is defined as the projection of tissue between stent struts with difficulty to differentiate from thrombus in the consensus document [17]. CAS can distinguish between plaque and thrombus through a direct visualization of the intracoronary structure. A previous CAS study have revealed that IP was associated with yellow plaque and thrombus was observed in 69% of lesions with OCT-detected IP [18]. Furthermore, underlying lipid-rich plaque and thrombus have been OCT predictors of IP [7]. These findings indicate that IP generally consists of lipid plaque and/or thrombus protruding between stent struts after strut penetration into a necrotic core. Since CAS showed that all residual IP at 1 month were composed of yellow plaques with red thrombi in the current study, these CAS findings are consistent with the appearance of IP which the previous CAS study reported [18].

The incidence of IP immediately after the initial PCI was 35.5% in this study including only CCS patients, whereas the incidence of IP was reported to be 80% in the culprit lesions in patients with ST-segment elevation myocardial infarction [19]. The difference can be explained by the plaque morphology underlying lesions associated with ACS and CCS: ACS lesions more frequently have lipid-rich plaque, which is an independent predictor of IP, compared with CCS lesions [7, 8]. A previous OCT study has demonstrated that tissue protrusion was less frequently observed after stent implantation in CCS and ACS patients (42% vs. 79%, $p = 0.005$). This result aligned with our results.

Regarding the consequence of tissue protrusion, several OCT studies have revealed that tissue protrusion, including not only IP, disappeared at 6–8 months after the PCI [3, 20]. Our study, including only IP, demonstrated that most of them disappeared at 12 months as with the previous studies. Interestingly, 76.3% of IP already disappeared at 1 month. Pathological studies have shown that platelet/fibrin deposition and inflammatory cell accumulation occur as the earliest change following stent implantation. They decrease over time and are rarely observed beyond 1 month. Instead of them, smooth muscle cell migration and proliferation start before 1 month [21]. Additionally, thrombus in IP could be resolved by dual antiplatelet therapy. IP could usually disappear by 1 month via the vessel healing

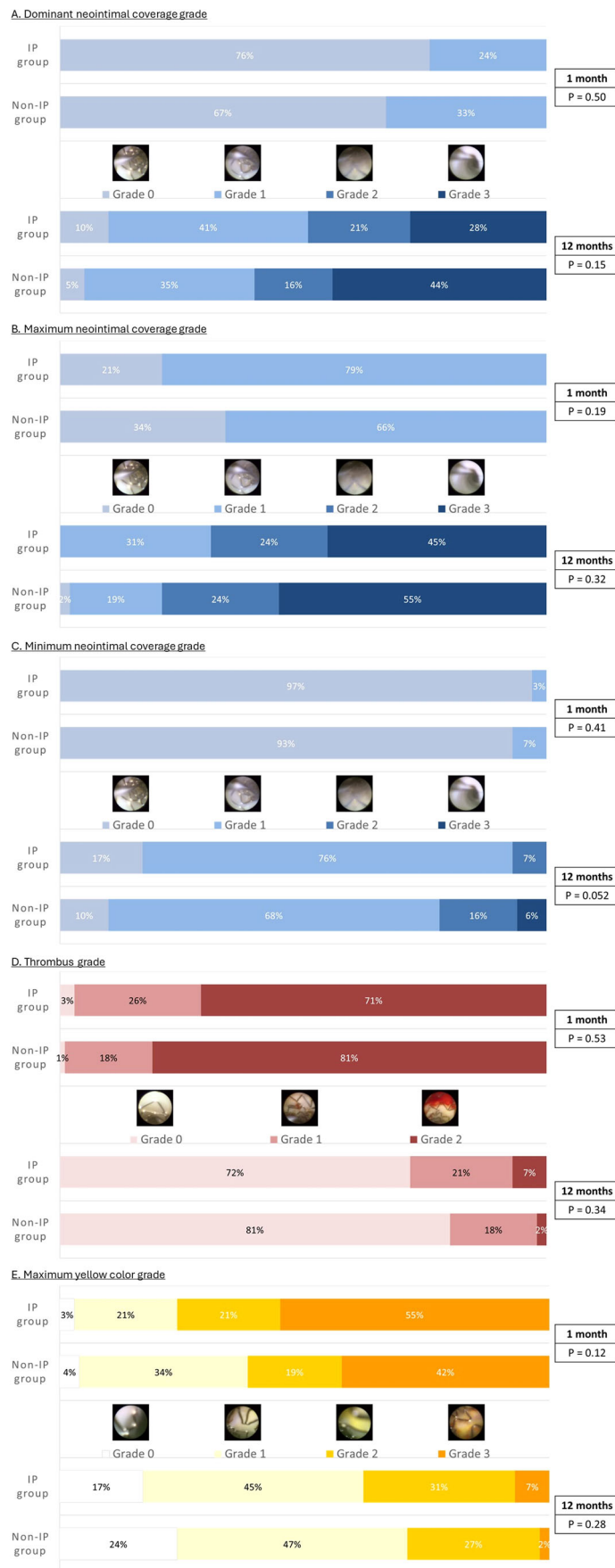


FIGURE 2 | Serial coronary angiographic findings at 1 month and 12 months. (A) Dominant neointimal coverage grade. (B) Maximum neointimal coverage grade. (C) Minimum neointimal coverage grade. (D) Thrombus grade. (E) Maximum yellow color grade. [Color figure can be viewed at [wileyonlinelibrary.com](https://onlinelibrary.wiley.com)]

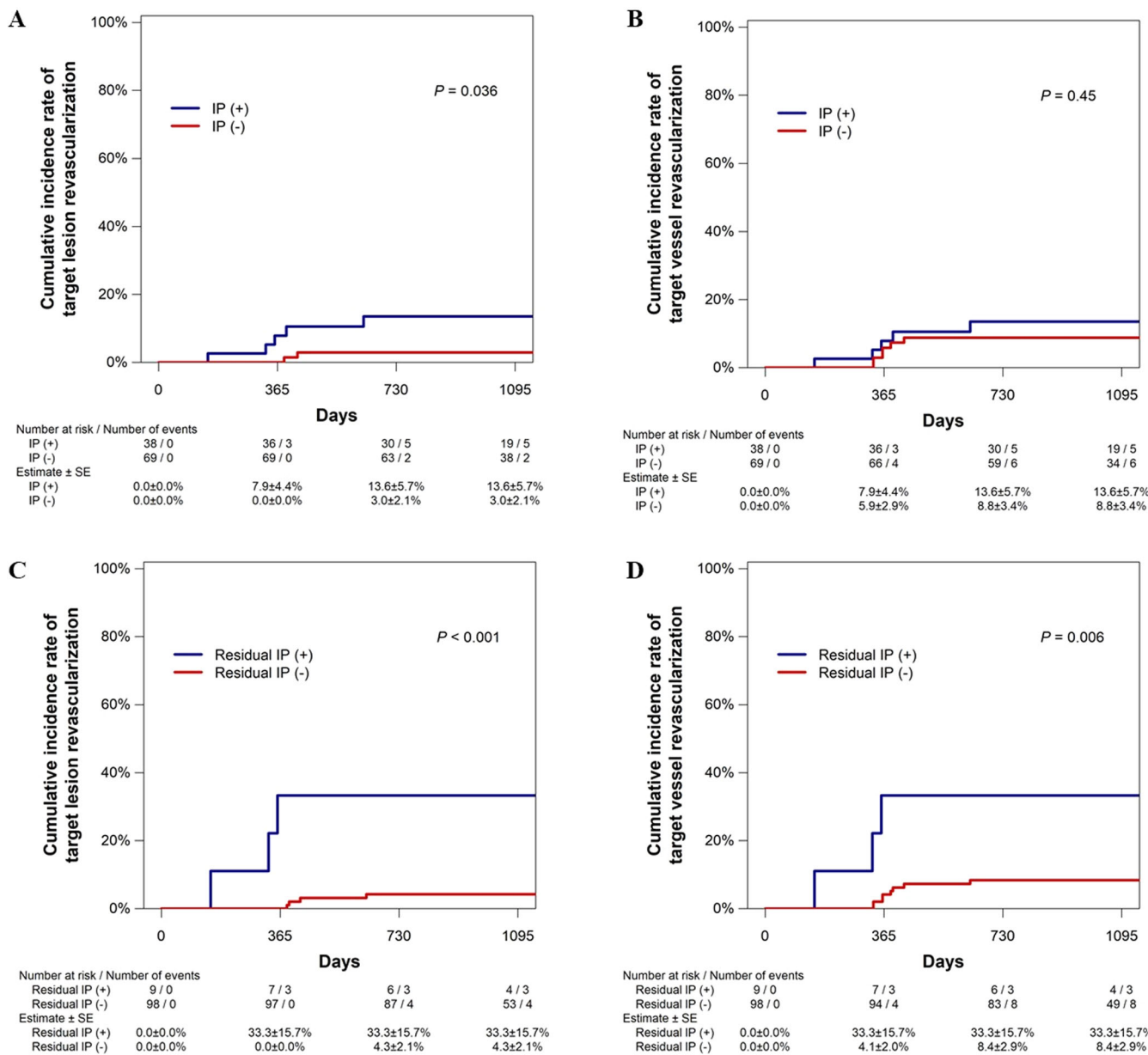


FIGURE 3 | Three-year clinical outcomes. (A and B) Show cumulative incident rates of target lesion revascularization and target vessel revascularization according to the presence of irregular protrusion immediately after stent implantation. (C and D) Demonstrate cumulative incident rates of target lesion revascularization and target vessel revascularization in lesions with or without residual irregular protrusion at 1 month. [Color figure can be viewed at [wileyonlinelibrary.com](https://onlinelibrary.wiley.com)]

process. However, approximately one-fourth of IP still existed at 1 month. Our CAS findings of the residual IP at 1 month were a combination of yellow plaque and red thrombus similar to the reported CAS findings of IP immediately after stent implantation [18]. It has been reported that the vessel healing process after stent implantation completes around 18 months after bare-metal stent implantation and it can be delayed after DES implantation [21, 22]. Furthermore, a pathological study has shown that strut penetration into a necrotic core delays vessel healing after DES implantation [23]. Considering the nature of IP, lesions with IP could be likely to have delayed vessel healing. Our 1-month follow-up OCT demonstrated that signal patterns of neointima were different between the lesions with or without IP. The pathological meanings of neointima with high- or low-signal pattern at 1 month after stent implantation are

difficult to conclude because neointimal growth is just beginning at that time [21]. However, the different signal patterns might suggest the different speeds of the vessel healing process according to the presence of IP.

Soeda et al. have reported that IP is an independent predictor of 1-year TLR. 49.5% of the included patients ($n = 727$) had ACS in the report. In such a patient population, 1-year TLR was 5.8% in lesions with IP versus 1.8% in lesions without IP with an odds ratio of 2.66 (95% confidence interval 1.40%–5.05%, $p < 0.01$). However, there has been no data regarding clinical outcomes beyond 1 year, nor is it limited only in CCS. This study first demonstrated that IP was an important finding to determine long-term TLR in patients with CCS. Previous pathological papers have demonstrated that the embedded struts in deep

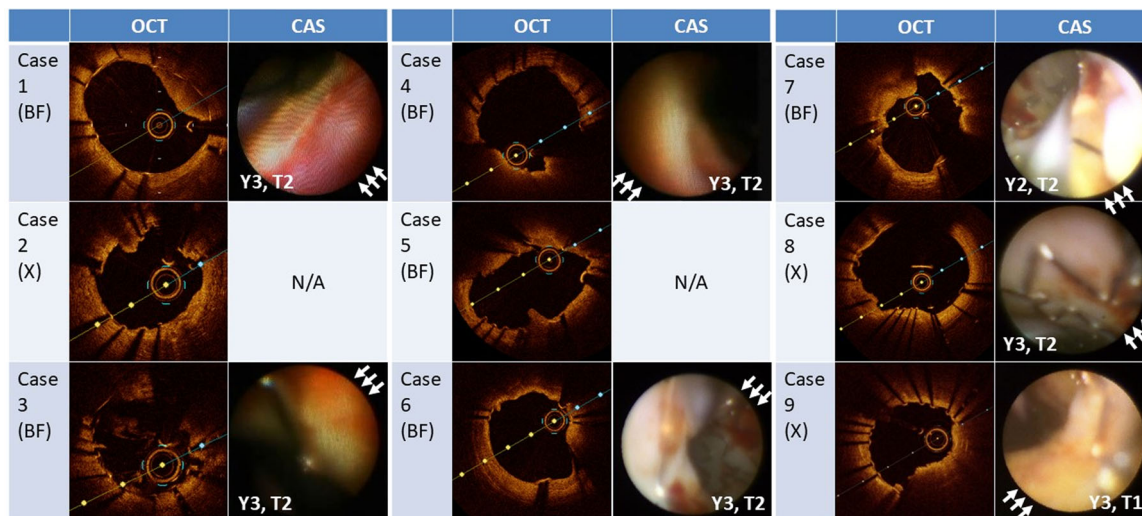


FIGURE 4 | Optical coherence tomography and coronary angiography images of residual irregular protrusion at 1 month. White arrows indicate irregular protrusion observed in coronary angiography. Y indicates yellow color grade and T means thrombus grade for each angiography image. BF refers to BioFreedom, and X represents Xience. [Color figure can be viewed at wileyonlinelibrary.com]

vessel injury to the media by stent implantation enhance arterial inflammation and thrombogenicity, which could cause in-stent restenosis and stent thrombosis [24, 25]. This study revealed that struts were more deeply embedded in IP group than in non-IP group. This finding might explain the greater incidence of TLR in lesions with IP compared with those without. Additionally, several studies have demonstrated that IP is associated with subsequent neoatherosclerosis [26, 27], although there was no significant difference in the presence of neoatherosclerosis at 12-month OCT examinations between IP and non-IP groups (7% vs. 6%, $p > 0.99$) in the current study. It has been shown that neoatherosclerosis developing more than 1 year after stent implantation is associated with poor long-term clinical outcomes, including TLR [28]. Neoatherosclerosis, which likely develops in lesions with IP, could be associated with a 3-year higher rate of TLR in lesions with IP.

Furthermore, the residual IP at 1 month was strongly related to both 3-year TLR and TVR. Residual IP might have not only enhanced inflammation and thrombogenicity but also delayed vessel healing as mentioned above. These features of residual IP might cause a strong association between the residual IP and adverse clinical outcomes. However, further investigations regarding the predictors of residual IP, especially noninvasive predictors, are warranted since residual IP is difficult to detect in daily practice due to the impracticality of routine serial invasive imaging. A multivariable analysis was conducted to identify independent predictors of residual IP using variables that showed significant differences between the residual IP and non-residual IP groups (Tables 5 and 6). The right coronary artery, pre-percent diameter stenosis, and stent size were identified as independent predictors of residual IP. It is possible that implanting oversized stents in a vessel with a large plaque burden may contribute to residual IP. However, the number of lesions with residual IP was too small to draw a definitive conclusion.

IP can be detected by OCT, whereas it is challenging to detect it using intravascular ultrasound (IVUS) due to its low resolution.

This study demonstrated that IP is associated with long-term TLR in patients with CCS. From this perspective, OCT offers an advantage in detecting prognostic findings compared to IVUS. Long-term and careful clinical follow-up is necessary for patients with IP after stent implantation. While prevention of IP is ideal, managing its incidence remains difficult. Recently, long inflation with a perfusion balloon has been shown to reduce the maximum protrusion area measured by OCT in patients with ST-segment elevated myocardial infarction [29]. This strategy may also be effective for lipid-rich and/or thrombotic lesions, even in patients with CCS.

4.1 | Study Limitations

The lack of pre-OCT data on underlying plaque characteristics is a significant limitation, since lipid-rich plaque can confound the incidence of IP. The TLR and TVR rates in our study was comparable to those reported in the previous studies [30, 31]. However, given the small number of TLR and TVR events, caution is warranted in interpreting the study results.

5 | Conclusion

The presence of IP decreased over time after stent implantation, but approximately one-fourth of IP remained at 1 month. IP was an important post-stent OCT finding leading to long-term TLR in patients with CCS. Furthermore, the residual IP at 1 month was strongly associated with both long-term TLR and TVR (Central_Illustration 1).

6 | Impact on Daily Practice

This study shows that IP was an important post-stent OCT finding leading to 3-year TLR in patients with CCS. The presence of IP decreased over time after stent implantation, but

TABLE 5 | Patient, lesion, and procedural characteristics between lesions with and without residual IP at 1 month.

	Residual IP group (n = 9)	Non-residual IP group (n = 98)	p value
Age	77 (71.5–82)	73 (68–78.3)	0.21
Male, n (%)	8 (89)	83 (85)	1.00
Current smoker, n (%)	1 (11)	29 (30)	0.44
Hypertension, n (%)	8 (89)	75 (77)	0.68
Dyslipidemia, n (%)	9 (100)	94 (96)	1.00
Diabetes mellitus, n (%)	3 (33)	46 (47)	0.50
Prior percutaneous coronary intervention, n (%)	3 (33)	31 (32)	1.00
Prior coronary artery bypass graft, n (%)	1 (11)	4 (4)	0.36
Atrial fibrillation, n (%)	1 (11)	14 (14)	1.00
Chronic heart disease, n (%)	2 (22)	6 (6)	0.14
Cerebral vascular disease, n (%)	0 (0)	13 (13)	0.60
Medication use at the time of initial percutaneous coronary intervention, n (%)			
Aspirin	9 (100)	98 (100)	
P2Y12 inhibitor			1.00
Clopidogrel	3 (33)	29 (30)	
Prasugrel	6 (67)	69 (70)	
Anticoagulant	1 (11)	13 (13)	0.85
Statin	9 (100)	89 (91)	1.00
Presence of symptoms, n (%)	6 (67)	53 (54)	0.73
Triple vessel disease, n (%)	1 (11)	22 (2)	0.69
Target vessel, n (%), LAD/LCX/RCA	1 (11)/1 (11)/7 (78)	31 (32)/38 (39)/29 (30)	0.01
Chronic total occlusion, n (%)	3 (33)	2 (2)	0.004
Lesion length, mm	22 (11.5–35.5)	23 (13.3–32)	0.87
Pre-reference vessel diameter, mm	2.8 (2.15–3.45)	2.60 (2.20–3.00)	0.43
Pre minimum lumen diameter, mm	0.30 (0–1.2)	0.80 (0.60–1.10)	0.13
Pre percent diameter stenosis, %	86.4 (69.0–100)	66.7 (58.2–75.3)	0.01
AHA/ACC classification, n (%), A/B1/B2/C	0 (0)/1 (11)/0 (0)/8 (89)	6 (6)/11 (11)/13 (13)/68 (69)	0.53
Number of stents	1 (1–2)	1 (1–1)	0.28
Biofreedom	6 (67)	54 (55)	0.73
Stent size, mm	3.50 (2.97–3.75)	2.71 (2.50–3.00)	0.002
Stent length, mm	28 (21–70)	28 (18–38)	0.43
Stent pressure, atm	6.5 (6–10.5)	8 (6–12)	0.62
Stent size/pre-RVD	1.19 (1.07–1.41)	1.09 (0.98–1.22)	0.08
Predilation, n (%)	8 (89)	86 (88)	0.92
Pre-balloon size, mm	2.75 (2.13–3.19)	2.5 (2–2.75)	0.23
Pre-balloon pressure, atm	12 (12–14)	12 (10–14)	0.49
Postdilation, n (%)	8 (88)	96 (98)	0.11
Post balloon size, mm	3.75 (3.5–4.0)	3.13 (2.75–3.5)	0.005
Post balloon pressure, atm	18 (12.5–18)	18 (18–20)	0.18

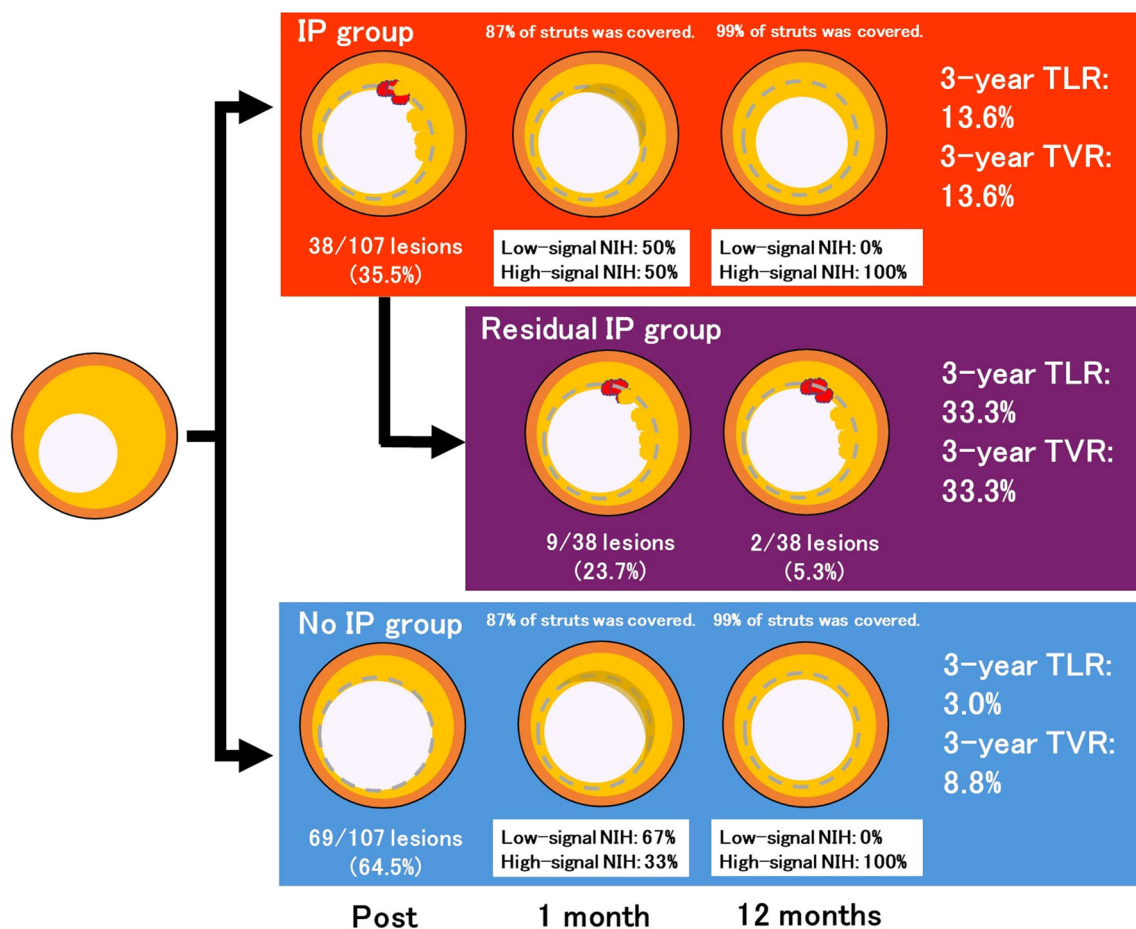
Note: Values are the median (interquartile) or n (%).

Abbreviations: IP = irregular protrusion, LAD = left anterior descending artery, LCX = left circumflex, RCA = right coronary artery, RVD = reference vessel diameter.

TABLE 6 | Independent factors of the residual irregular protrusion.

	Univariable			Multivariable		
	Odd's ratio	95% CI	<i>p</i> value	Odd's ratio	95% CI	<i>p</i> value
Right coronary artery	8.33	1.63–42.51	0.01	5.12	0.69–37.72	0.11
Chronic total occlusion	24.00	3.34–172.12	0.002			
Pre percent diameter, %	1.09	1.03–1.15	0.002	1.14	1.04–1.24	0.0003
Stent size, mm	16.21	2.79–94.06	0.002	55.4	3.13–979.8	0.006
Postdilatation balloon size, mm	8.75	1.78–42.98	0.008			

Abbreviation: CI = confidence interval.



CENTRAL_ILLUSTRATION 1 | The presence of irregular protrusion (IP) decreased over time after stent deployment in chronic coronary syndrome. At 1 month, 23.7% of IP remained. IP was significantly associated with 3-year target lesion revascularization. Furthermore, residual IP at 1 month was strongly associated with 3-year target lesion revascularization and target vessel revascularization. [Color figure can be viewed at [wileyonlinelibrary.com](https://onlinelibrary.wiley.com)]

approximately one-fourth of IP remained at 1 month. The residual IP at 1 month was strongly associated with both 3-year TLR and TVR.

Kazuya Shinouchi for their expertise in OCT analysis; and Ms. Saori Kashu and Ms. Akiko Abe for their expertise in data aggregation. This study was supported by Abbott Medical Japan, Cardinal Health Japan, Taisho Biomed Instruments Co. Ltd. and Biosensors Japan.

Acknowledgments

We wish to thank Drs. Taku Toyoshima, Naoko Higashino, and Sho Nakao for their expertise in data collection; Mr. Naoya Kurata, Mr. Takashi Sumikawa, Mr. Hiroki Oyama, Mr. Kazutoshi Ito, Mr. Yusuke Katagiri, Mr. Kohei Nanri, and Ms. Haruna Miyaguchi for their expertise in performing CAS and OCT examinations; Mr. Yuji Kiyose, Mr. Tomohiro Yamanaka, Dr. Bolrathanak Oeun, and Dr.

Conflicts of Interest

N.O. has received lecture fees from Abiomed Japan and Boston Scientific Japan. I.M. has received a scholarship fund from Abbott Medical Japan. T.M. has received a research grant from Abbott Medical Japan. M.N. receives donations from Abbott Medical Japan, Boston Scientific Japan, Medtronic, and Japan Lifeline. Y.S. has received a scholarship fund from Abbott Medical Japan.

Data Availability Statement

Our study data will not be made available to other researchers for purposes of reproducing the results because of institutional review board restrictions.

References

1. I. K. Jang, G. Tearney, and B. Bouma, "Visualization of Tissue Prolapse Between Coronary Stent Struts by Optical Coherence Tomography: Comparison With Intravascular Ultrasound," *Circulation* 104 (2001): 2754.
2. N. Gonzalo, P. W. Serruys, T. Okamura, et al., "Optical Coherence Tomography Assessment of the Acute Effects of Stent Implantation on the Vessel Wall: A Systematic Quantitative Approach," *Heart* 95 (2009): 1913–1919.
3. H. Kawamori, J. Shite, T. Shinke, et al., "Natural Consequence of Post-Intervention Stent Malapposition, Thrombus, Tissue Prolapse, and Dissection Assessed by Optical Coherence Tomography at Mid-Term Follow-Up," *European Heart Journal-Cardiovascular Imaging* 14 (2013): 865–875.
4. T. Kubo, T. Imanishi, H. Kitabata, et al., "Comparison of Vascular Response After Sirolimus-Eluting Stent Implantation Between Patients With Unstable and Stable Angina Pectoris," *JACC: Cardiovascular Imaging* 1 (2008): 475–484.
5. T. Sugiyama, S. Kimura, D. Akiyama, et al., "Quantitative Assessment of Tissue Prolapse on Optical Coherence Tomography and Its Relation to Underlying Plaque Morphologies and Clinical Outcome in Patients With Elective Stent Implantation," *International Journal of Cardiology* 176 (2014): 182–190.
6. T. Soeda, S. Uemura, S. J. Park, et al., "Incidence and Clinical Significance of Poststent Optical Coherence Tomography Findings: One-Year Follow-Up Study From a Multicenter Registry," *Circulation* 132 (2015): 1020–1029.
7. K. Bryniarski, S. J. Tahk, S. Y. Choi, et al., "Clinical, Angiographic, IVUS, and OCT Predictors for Irregular Protrusion After Coronary Stenting," *EuroIntervention* 12 (2017): e2204–e2211.
8. I. K. Jang, G. J. Tearney, B. MacNeill, et al., "In Vivo Characterization of Coronary Atherosclerotic Plaque by Use of Optical Coherence Tomography," *Circulation* 111 (2005): 1551–1555.
9. K. Kimura, T. Kimura, M. Ishihara, et al., "JCS 2018 Guideline on Diagnosis and Treatment of Acute Coronary Syndrome," *Circulation Journal* 83 (2019): 1085–1196.
10. S. Kuramitsu, M. Ohya, T. Shinozaki, et al., "Risk Factors and Long-Term Clinical Outcomes of Second-Generation Drug-Eluting Stent Thrombosis," *Circulation: Cardiovascular Interventions* 12 (2019): e007822.
11. T. Ishihara, I. Mizote, D. Nakamura, et al., "Comparison of 1-Month and 12-Month Vessel Responses Between the Polymer-Free Biolimus A9-Coated Stent and the Durable Polymer Everolimus-Eluting Stent," *Circulation Journal* 86 (2022): 1397–1408.
12. T. Tada, K. Kadota, S. Hosogi, et al., "Association Between Tissue Characteristics Evaluated With Optical Coherence Tomography and Mid-Term Results After Paclitaxel-Coated Balloon Dilatation for In-Stent Restenosis Lesions: A Comparison With Plain Old Balloon Angioplasty," *European Heart Journal-Cardiovascular Imaging* 15 (2014): 307–315.
13. T. Ishihara, T. Tsujimura, S. Okuno, et al., "Early- and Middle-Phase Arterial Repair Following Bioresorbable- and Durable-Polymer Drug-Eluting Stent Implantation: An Angioscopic Study," *International Journal of Cardiology* 285 (2019): 27–31.
14. Y. Mitsutake, H. Yano, T. Ishihara, H. Matsuoka, Y. Ueda, and T. Ueno, "Consensus Document on the Standard of Coronary Angioscopy Examination and Assessment From the Japanese Association of Cardiovascular Intervention and Therapeutics," *Cardiovascular Intervention and Therapeutics* 37 (2022): 35–39.
15. K. Thygesen, J. S. Alpert, A. S. Jaffe, M. L. Simoons, B. R. Chaitman, and H. D. White, "Third Universal Definition of Myocardial Infarction," *Circulation* 126 (2012): 2020–2035.
16. D. E. Cutlip, S. Windecker, R. Mehran, et al., "Clinical End Points in Coronary Stent Trials: A Case for Standardized Definitions," *Circulation* 115 (2007): 2344–2351.
17. G. J. Tearney, E. Regar, T. Akasaka, et al., "Consensus Standards for Acquisition, Measurement, and Reporting of Intravascular Optical Coherence Tomography Studies," *Journal of the American College of Cardiology* 59 (2012): 1058–1072.
18. S. Sakai, A. Sato, T. Hoshi, D. Hiraya, H. Watabe, and M. Ieda, "In Vivo Evaluation of Tissue Protrusion by Using Optical Coherence Tomography and Coronary Angioscopy Immediately After Stent Implantation," *Circulation Journal* 84 (2020): 2235–2243.
19. A. Kyodo, T. Soeda, A. Okamura, et al., "Clinical Impact of Irregular Protrusion Angle After Coronary Stenting at Culprit Lesions With ST-Elevation Myocardial Infarction: An Intravascular Optical Coherence Tomography Study," *Circulation Reports* 3 (2021): 431–439.
20. T. Kume, H. Okura, Y. Miyamoto, et al., "Natural History of Stent Edge Dissection, Tissue Protrusion and Incomplete Stent Apposition Detectable Only on Optical Coherence Tomography After Stent Implantation: Preliminary Observation," *Circulation Journal* 76 (2012): 698–703.
21. M. Nakano and R. Virmani, "Histopathology of Vascular Response to Drug-Eluting Stents: An Insight From Human Autopsy Into Daily Practice," *Cardiovascular Intervention and Therapeutics* 30 (2015): 1–11.
22. M. Joner, A. V. Finn, A. Farb, et al., "Pathology of Drug-Eluting Stents in Humans," *Journal of the American College of Cardiology* 48 (2006): 193–202.
23. G. Nakazawa, A. V. Finn, M. Joner, et al., "Delayed Arterial Healing and Increased Late Stent Thrombosis at Culprit Sites After Drug-Eluting Stent Placement for Acute Myocardial Infarction Patients: An Autopsy Study," *Circulation* 118 (2008): 1138–1145.
24. A. Farb, G. Sangiorgi, A. J. Carter, et al., "Pathology of Acute and Chronic Coronary Stenting in Humans," *Circulation* 99 (1999): 44–52.
25. M. Nakano, K. Yahagi, F. Otsuka, et al., "Causes of Early Stent Thrombosis in Patients Presenting With Acute Coronary Syndrome," *Journal of the American College of Cardiology* 63 (2014): 2510–2520.
26. Y. Sanuki, S. Sonoda, Y. Muraoka, et al., "Contribution of Poststent Irregular Protrusion to Subsequent In-Stent Neoatherosclerosis After the Second-Generation Drug-Eluting Stent Implantation," *International Heart Journal* 59 (2018): 307–314.
27. K. Yanagawa, D. Nakamura, Y. Egami, et al., "Predictors for the Early Development of Neoatherosclerosis After Newer-Generation Drug-Eluting Stent Implantation an Optical Coherence Tomographic Study," *Journal of Coronary Artery Disease* 28 (2022): 78–86.
28. M. Kuroda, H. Otake, T. Shinke, et al., "The Impact of In-Stent Neoatherosclerosis on Long-Term Clinical Outcomes: An Observational Study From the Kobe University Hospital Optical Coherence Tomography Registry," *EuroIntervention* 12 (2016): e1366–e1374.
29. M. Nishino, Y. Egami, H. Nakamura, et al., "Clinical Impact of Perfusion Balloon for ST-Segment Elevated Myocardial Infarction: RYUSEI Study," *American Journal of Cardiology* 223 (2024): 43–51.
30. D. E. Kandzari, J. J. Koolen, G. Doros, et al., "Ultrathin Bioresorbable-Polymer Sirolimus-Eluting Stents Versus Thin Durable-Polymer Everolimus-Eluting Stents for Coronary Revascularization: 3-Year Outcomes From the Randomized BIOFLOW V Trial," *JACC Cardiovascular Interventions* 13 (2020): 1343–1353.
31. F. R. Eberli, K. G. Oldroyd, P. Urban, et al., "Clinical Outcomes With Thin Versus Thick Strut Polymer-Free Biolimus-Coated Stents at 3 Years," *Open Heart* 11 (2024): e002679.